Journal of Applied Fluid Mechanics, Vol. 9, No. 2, pp. 605-613, 2016.
Available online at www.jafmonline.net, ISSN 1735-3572, EISSN 1735-3645.
DOI: 10.18869/acadpub.jafm.68.225.24457

Entropy Generation Analysis for the Peristaltic Flow of Cu-water Nanofluid with Magnetic Field in a Lopsided Channel

N. Sher Akbar[1†] and Z. H. Khan[2]

[1] *DBS&H, CEME, National University of Sciences and Technology, Islamabad, Pakistan*
[2] *Department of Mathematics, University of Malakand, Chakdara, Dir (Lower), Khyber Pakhtunkhwa, Pakistan*

†*Corresponding Author Email*: *noreensher@yahoo.com*

(Received January 7, 2015; accepted February 24, 2015)

ABSTRACT

This article is intended for investigating the entropy generation analysis for the peristaltic flow of Cu-water nanofluid with magnetic field in a lopsided channel. The mathematical formulation is presented. The resulting equations are solved exactly. The obtained expressions for pressure gradient, pressure rise, temperature and velocity phenomenon are described through graphs for various pertinent parameters. The streamlines are drawn for some physical quantities to discuss the trapping phenomenon.

Keywords: Magnetic field; Peristaltic flow; Cu-Water; Lopsided channel.

1. INTRODUCTION

In the antiquity of fluid subtleties, the extent of peristaltic transference have gained momentous desirability due to its substantial influence in the arenas of manufacturing and biomechanics as this procedure remnants energetic in numerous organic devices and biomedical engineering. Unambiguously, it is extremely functional in the design of swallowing food through the esophagus, chyme motion in the gastrointestinal tract, vasomotion of small blood vessels such as venules, capillaries and arterioles, urine transport flow from kidney to bladder, sanitary fluid transportation, transportation of corrosive fluids and a toxic liquid flow in the nuclear industry etc. In the opinion of such huge influence of peristaltic movements in engineering and biomedical many researchers have absorbed on the study of peristaltic mechanism. Logically, the behavior of regularly used liquids in such type of phenomenons is typically non-Newtonian to concentrated degree. Custody in attention the difficulty of non-Newtonian fluids, numerous of the investigators have functioned on the peristaltic flows of dissimilar non-Newtonian models in the intelligence of constitutive relations. In the studies [1 – 6] , the scholars have gained the numerous results concerning peristaltic flows in different flow geometries.

In present-days nanofluid is a topic of innumerable courtesy among the researchers. Choi (1995) was the chief who have habituated the word "nanofluid" which elucidate a fluid rescheduling including ultrafine units with span less than 50 nm. The increase in thermal conductivity of nanofluids has been accredited to a volume of varied geniuses with Brownian motion, bunching of nanoparticles and fluid layering at the liquid/solid border. In peristaltic rhyme few studies have been completed for nano fluid. Akbar and Nadeem (2014) present endoscopic properties on the peristaltic flow of a nanofluid. In a further article Akbar *et al*. (2012) considered the peristaltic flow of a nanofluid in a non-uniform tube. Very recently Hamad and Ferdows (2012) explore the similarity solution of boundary layer stagnation-point flow towards a heated porous and nonlinear stretching sheet saturated with nano fluid with Cu-water nano fluid with water as base fluid.

In thermodynamics, entropy is a measure of the number of specific ways in which a thermodynamic system may be arranged, often taken to be a measure of disorder, or a measure of progressing towards thermodynamic equilibrium. Bejan (1979) studied the entropy generation in fundamental convective heat transfer. Non-Newtonian fluid flow in a pipe system with entropy generation is considered by Pakdemirli and Yilbas (2006). According to them entropy number increases with increasing Brinkman number. Entropy generation due to heat and fluid flow in backward facing step flow with various expansion ratios is studied by

Abu-Nada (2005). Further analysis could be seen through References.

Entropy generation for peristaltic flow is not explored so far, to fill this gap we have investigated the entropy generation analysis for the peristaltic flow of Cu-water nanofluid with magnetic field in a lopsided channel. The coupled differential equations are simplified under long wave length and low Reynolds number assumptions. Exact solutions are obtained for reduced coupled differential equations. The entropy generation is computed by evaluation of thermal and fluid viscosities contribution. The physical features of pertinent parameters have been discussed by plotting the graphs of velocity, temperature, entropy number and stream functions.

2. MATHEMATICAL FORMULATION

Let us discussed an incompressible Cu-water nanofluid in an asymmetric channel of width $d_1 + d_2$. The channel has a sinusoidal wave propagating with constant speed c on the channel walls induces the flow. The asymmetric of the channel is due to different amplitudes. Temperature $\overline{T}_0$, $\overline{T}_1$ and nanoparticle concentrations $\overline{C}_0$, $\overline{C}_1$ are given to the upper and lower wall of the channel. The wall surfaces are selected to satisfy the following expressions

$$\begin{aligned} Y = H_1 &= d_1 + a_1 \cos\left[\frac{2\pi}{\lambda}(X - ct)\right], \\ Y = H_2 &= -d_2 - b_1 \cos\left[\frac{2\pi}{\lambda}(X - ct) + \phi\right]. \end{aligned} \tag{1}$$

In the above equations a_1 and b_1 are the waves amplitudes, λ is the wave length, $d_1 + d_2$ is the channel width, c_1 is the wave speed, t is the time, X is the direction of wave propagation and Y is perpendicular to X. The phase difference ϕ varies in the range $0 \le \phi \le \pi$. When $\phi = 0$ then symmetric channel with waves out of phase can be described and for $\phi = \pi$, the waves are in phase. Moreover, a_1, b_1, d_1, d_2 and ϕ satisfies the following relation

$$a_1^2 + b_1^2 + 2a_1 b_1 \cos\phi \le (d_1 + d_2)^2.$$

The coordinates, velocity components and pressure between fixed and wave frames are related by the following transformations:,

$$\bar{x} = \overline{X} - ct,\ \bar{y} = \overline{Y},\ \bar{u} = \overline{U} - c,\ \bar{v} = \overline{V},\ p(\bar{x}) = P(\overline{X}, t), \tag{2}$$

in which $(\bar{x}, \bar{y})$, $(\bar{u}, \bar{v})$ and $\bar{p}$ are the coordinates, velocity components and pressure in the wave frame.

With the transformation given Eq. (2) equations governing the flow and temperature in the presence of heat source or heat sink with viscous dissipation are

$$\frac{\partial \bar{u}}{\partial \bar{x}} + \frac{\partial \bar{v}}{\partial \bar{y}} = 0, \tag{3}$$

$$\begin{aligned} \bar{u}\frac{\partial \bar{u}}{\partial \bar{x}} + \bar{v}\frac{\partial \bar{u}}{\partial \bar{y}} &= -\frac{1}{\rho_{nf}}\frac{\partial P}{\partial \bar{x}} + \frac{\mu_{nf}}{\rho_{nf}}\frac{\partial^2 \bar{u}}{\partial \bar{y}^2} + \frac{\mu_{nf}}{\rho_{nf}}\frac{\partial^2 \bar{u}}{\partial \bar{x}^2} \\ &\quad - \frac{\sigma B_o^2}{\rho_{nf}}(\bar{u} + c_1), \end{aligned} \tag{4}$$

$$\bar{u}\frac{\partial \bar{v}}{\partial \bar{x}} + \bar{v}\frac{\partial \bar{v}}{\partial \bar{y}} = -\frac{1}{\rho_{nf}}\frac{\partial P}{\partial \bar{y}} + \frac{\mu_{nf}}{\rho_{nf}}\frac{\partial^2 \bar{v}}{\partial \bar{y}^2} + \frac{\mu_{nf}}{\rho_{nf}}\frac{\partial^2 \bar{v}}{\partial \bar{x}^2}, \tag{5}$$

$$\begin{aligned} \bar{u}\frac{\partial \overline{T}}{\partial \bar{x}} + \bar{v}\frac{\partial \overline{T}}{\partial \bar{y}} &= \alpha_{nf}\left(\frac{\partial^2 \overline{T}}{\partial \bar{y}^2} + \frac{\partial^2 \overline{T}}{\partial \bar{x}^2}\right) \\ &\quad + \frac{\mu_{nf}}{(\rho c_p)_{nf}}\left(\frac{\partial \bar{u}}{\partial \bar{y}} + \frac{\partial \bar{v}}{\partial \bar{x}}\right)^2, \end{aligned} \tag{6}$$

where $\bar{x}$ and $\bar{y}$ are the coordinates along and perpendicular to the channel, $\bar{u}$ and $\bar{v}$ are the velocity components in the $\bar{x}-$ and $\bar{y}-$ directions, respectively, $\overline{T}$ is the local temperature of the fluid. Further, ρ_{nf} is the effective density, μ_{nf} is the effective dynamic viscosity, $(\rho c_p)_{nf}$ is the heat capacitance, α_{nf} is the effective thermal diffusivity, and k_{nf} is the effective thermal conductivity of the nanofluid, which are defined as

$$\begin{aligned} &\rho_{nf} = (1-\phi)\rho_f + \phi\rho_f,\ \mu_{nf} = \frac{\mu_f}{(1-\phi)^{2.5}}, \\ &(\rho c_p)_{nf} = (1-\phi)(\rho c_p)_f + \phi(\rho c_p)_s,\ \alpha_{nf} = \frac{k_{nf}}{(\rho c_p)_{nf}}, \\ &k_{nf} = k_f\left(\frac{k_s + 2k_f - 2\phi(k_f - k_s)}{k_s + 2k_f + 2\phi(k_f - k_s)}\right) \end{aligned} \tag{7}$$

where ϕ is the solid volume fraction of the nanoparticles.

we introduce the following non-dimensional quantities

$$\begin{aligned} &x = \frac{2\pi\bar{x}}{\lambda},\ y = \frac{\bar{y}}{d_1},\ u = \frac{\bar{u}}{c},\ v = \frac{\bar{v}}{c},\ t = \frac{2\pi\bar{t}}{\lambda},\ \delta = \frac{2\pi d_1}{\lambda}, \\ &h_1 = \frac{\bar{h}_1}{d_1},\ h_2 = \frac{\bar{h}_2}{d_2}, \mathrm{Re} = \frac{\rho c d_1}{\mu_f}, a = \frac{a_1}{d_1}, b = \frac{a_2}{d_1}, S = \frac{\bar{S} d_1}{\mu_f c}, \\ &\theta = \frac{\overline{T} - \overline{T}_0}{\overline{T}_1 - \overline{T}_0},\ E_c = \frac{c^2}{(\overline{T}_1 - \overline{T}_0)(c_p)}, d = \frac{d_2}{d_1},\ P = \frac{2\pi d_1^2 P}{\mu_f c\lambda}, \\ &P_r = \frac{c_p \mu_f}{k_f}. \end{aligned} \tag{8}$$

in above equations P_r is the Prandtl number, M is Hartmann number and E_c is the Eckert number.

Stream function and velocity field are related by the expressions

$$u=\frac{\partial \Psi}{\partial y},\ v=-\delta\frac{\partial \Psi}{\partial x}, \tag{9}$$

In view of the Eqs. $(7-9)$ under the long wavelength and low Reynolds number assumption we have the following equations

$$\left(\frac{\mu_{nf}}{\mu_f}\right)\frac{\partial^4\Psi}{\partial y^4}-M^2\frac{\partial^2\Psi}{\partial y^2}=0, \tag{10}$$

$$\frac{dP}{dx}=\frac{\partial}{\partial y}\left[\left(\frac{\mu_{nf}}{\mu_f}\right)\frac{\partial^2\Psi}{\partial y^2}-M^2\left(\frac{\partial\Psi}{\partial y}+1\right)\right], \tag{11}$$

$$\left(\frac{k_{nf}}{k_f}\right)\frac{\partial^2\theta}{\partial y^2}+B_r\left(\frac{\mu_{nf}}{\mu_f}\right)\left(\frac{\partial^2\Psi}{\partial y^2}\right)^2=0, \tag{12}$$

The non-dimensionaless boundary conditions

$$\Psi=\frac{F}{2},\ \frac{\partial\Psi}{\partial y}=-1,\ \theta=0 \text{ at } y=h_1=1+a\cos x,$$

$$\Psi=-\frac{F}{2},\ \frac{\partial\Psi}{\partial y}=-1,\ \theta=1,\ \text{at } y=h_2=-d-b\cos(x+\varepsilon),$$

The flow rates in fixed and wave frame are related by

$$Q=F+1+d. \tag{13}$$

3. VISCOUS DISSIPATION AND ENTROPY GENERATION

The dimensional viscous dissipation term $\overline{\Phi}$ can be obtained from equations of motion, i.e,

$$\overline{\Phi}=\mu_{nf}\left(2\left(\left(\frac{\partial\bar{u}}{\partial\bar{x}}\right)^2+\left(\frac{\partial\bar{v}}{\partial\bar{y}}\right)^2\right)+\left(\frac{\partial\bar{u}}{\partial\bar{y}}+\frac{\partial\bar{v}}{\partial\bar{x}}\right)^2\right), \tag{14}$$

The dimensional volumetric entropy generation is defined as

$$S'''_{gen}=\frac{k_{nf}}{\bar{\theta}_0^2}\left(\left(\frac{\partial\bar{T}}{\partial\bar{x}}\right)^2+\left(\frac{\partial\bar{T}}{\partial\bar{y}}\right)^2\right)+\frac{\overline{\Phi}}{\bar{\theta}_0}, \tag{15}$$

Dimensionless form of the Entropy Generation in terms of stream function is given as:

$$Ns=\frac{S'''_{gen}}{S'''_G}=\left(\frac{k_{nf}}{k_f}\right)\left(\frac{\partial\theta}{\partial y}\right)^2+\Lambda B_r\left(\frac{\mu_{nf}}{\mu_f}\right)\left(\frac{\partial\Psi}{\partial y}\right)^2, \tag{16}$$

where

$$S'''_G=\frac{k_f\left(\bar{T}_1-\bar{T}_0\right)^2}{\bar{\theta}_0^2 d_1^2},\ B_r=\frac{c^2\mu_f}{k_f\left(\bar{T}_1-\bar{T}_0\right)},$$

$$\Lambda=\frac{\bar{\theta}_0}{\left(\bar{T}_1-\bar{T}_0\right)}.$$

$\bar{\theta}_0$ the reference temperature.

Equation (16) consists of two parts. The first part is the entropy generation due to finite temperature difference (Nscond) and the second part is the entropy generation due to viscous effects (Nsvisc). The Bejan number is defined as

$$B_e=\frac{Ns_{cond}}{Ns_{cond}+Ns_{visc}}. \tag{17}$$

4. SOLUTION PROFILES

Exact solutions for stream function, temperature profile using Mathematica 9 can be written as

$$\Psi(x,y)=c_3\sinh\left(\frac{My}{\sqrt{L}}\right)-c_4\sinh\left(\frac{My}{\sqrt{L}}\right)+c_3\cosh\left(\frac{My}{\sqrt{L}}\right)+c_4\cosh\left(\frac{My}{\sqrt{L}}\right)-\frac{c_1y}{M^2}-\frac{c_2}{M^2}, \tag{18}$$

$$\theta(x,y)=-\frac{Br\left(\frac{k_f}{k_{nf}}\right)M^3\left(\begin{array}{l}\frac{\left(c_3^2-c_4^2\right)L\sinh\left(\frac{2My}{\sqrt{L}}\right)}{2M}\\+\frac{\left(c_3^2+c_4^2\right)L\cosh\left(\frac{2My}{\sqrt{L}}\right)}{2M}\\+2c_3c_4My^2\end{array}\right)}{2L}+c_6y+c_5,\quad L=\left(\frac{\mu_{nf}}{\mu_f}\right). \tag{19}$$

where c_1-c_6 are constants evaluated using Mathematica 9.

The pressure rise Δp in non-dimensional form is defined as

$$\Delta P=\int_0^1\frac{dp}{dx}dx. \tag{20}$$

5. RESULTS AND DISCUSSION

In this section, we present a brief graphical analysis of the exact analytical solutions of the governing problem. Fig. $1(a)$ and $1(b)$ represent the magnitude of the horizontal velocity of the fluid inside the channel. We see that with the increase in the Hartmann number M , i.e. ratio of electromagnetic force to the viscous force, the

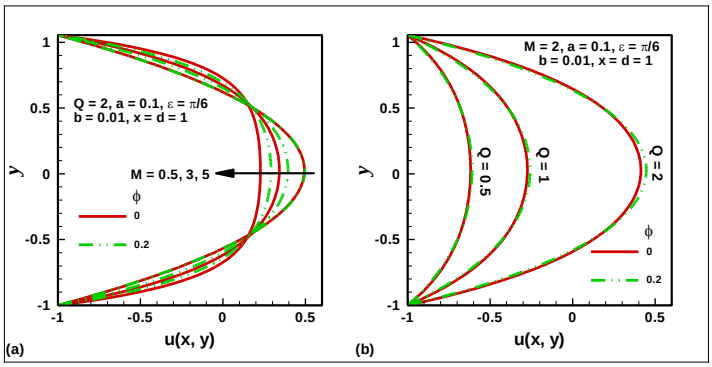

Fig. 1: Velocity profile a) different M and b) different Q.

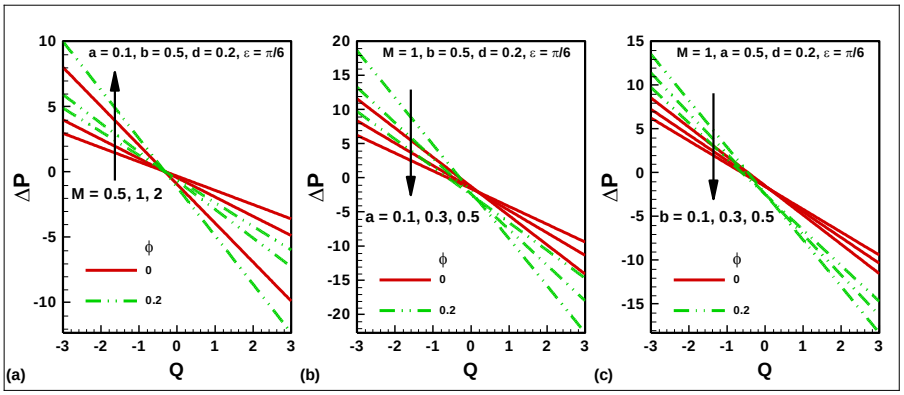

Fig. 2: Pressure rise ΔP for a) different M, b) different a and c) different b.

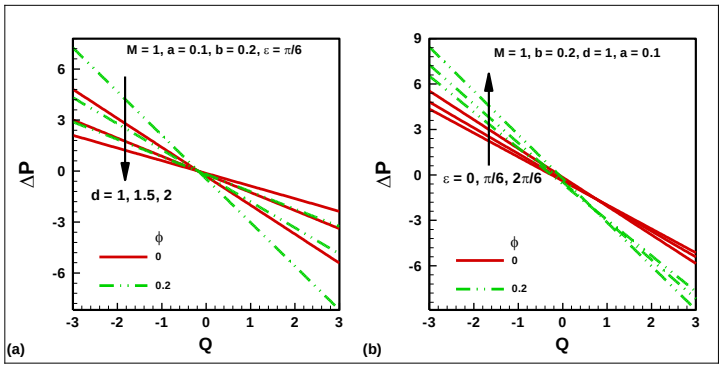

Fig 3: Pressure rise ΔP for a) different d and b) different ε

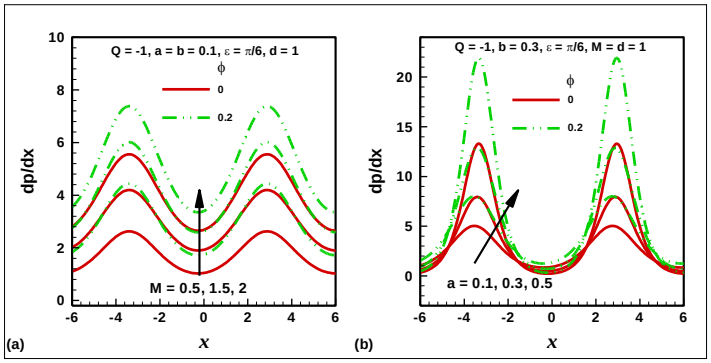

Fig. 4: Pressure gradient $\frac{dP}{dx}$ for a) different M and for different a.

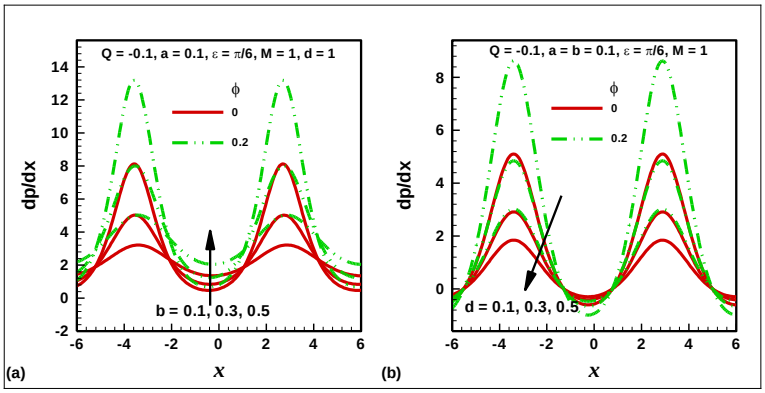

Fig. 5: Pressure gradient $\frac{dP}{dx}$ for a) different b and b) different d.

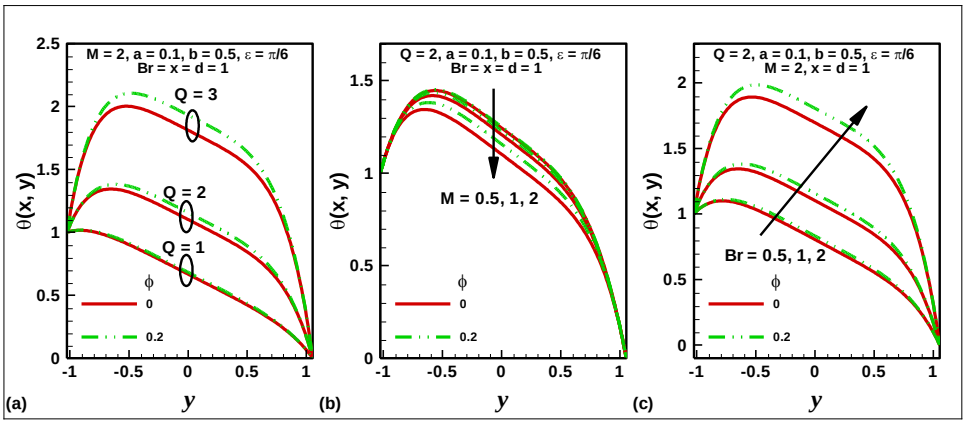

Fig. 6: Temperature profile for a) different Q, b) different M and c) different Br.

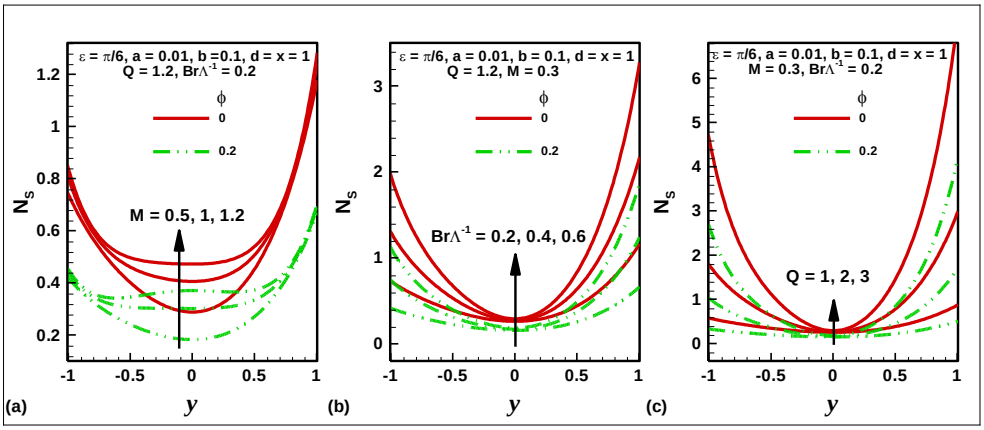

Fig. 7: Entropy generation number for a) different M, b) different $Br\Lambda^{-1}$ and c) different Q.

velocity decreases in the center of the tube and increases near the walls of the tube, while as we increase the flow rate Q , the magnitude of velocity takes a positive shift all around the tube. In both cases, it is observed that Cu-water has more variation as that of pure water. Also we note that the velocity attains its highest values in the center of the channel at $y = 0$, while it sufficiently decreases at the walls of the channel. Figs. $2(a)$ to $3(b)$ depict that with the addition of copper to the base fluid, the pressure rise gradually increases with the increase in Hartmann number M and amplitude ε while decreases with the increase in amplitudes ratio a, b and d in the peristaltic pumping region $\Delta P \succ 0$, while in the augmented pumping region $\Delta P \prec 0$ results are opposite pressure rise gradually decreases with the increase in Hartmann number M and amplitude ε while increases with the increase

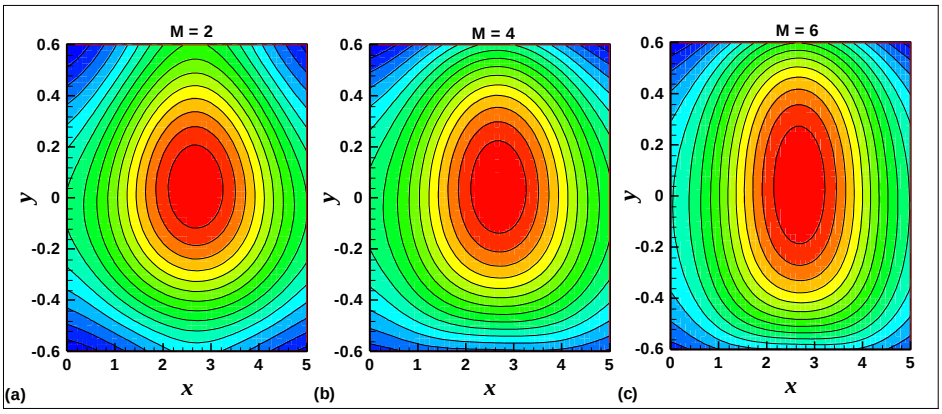

Fig. 8: Entropy generation number for a) M=2, b) M=4 and c) M=6.

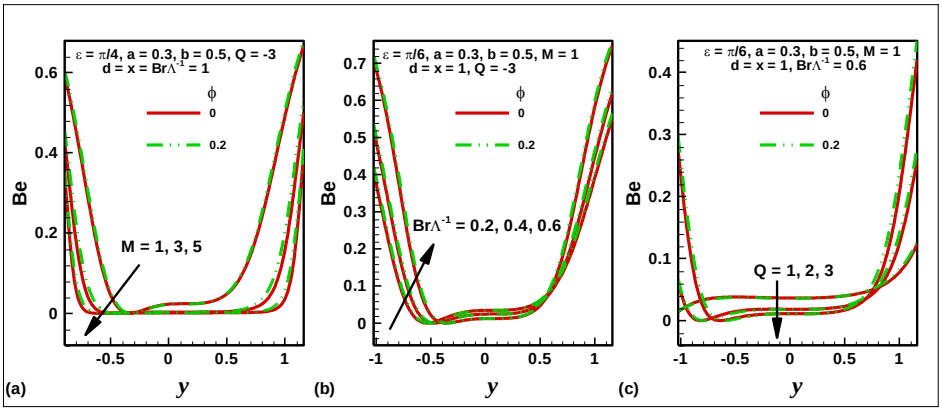

Fig. 9: Bejan number for different a) M, b) different $Br\Lambda^{-1}$ and c) different Q.

in amplitudes ratio a and b. Free pumping hold for $\Delta P = 0$. It is observed that pressure rise for Cu-water has more variation as compare to pure water. We note that the pressure gradient certainly increases with an increase in the Hartmann number, amplitudes a and b but pressure gradient decreases with the rise in amplitude d for both pure and Cu-water see Figs.5 (a) to 6 (b).

Temperature of the fluid in the tube significantly increases with an increase in flow rate Q and Brinkman number B_r and a decrease in Hartmann number M. However with less copper in the fluid, the temperature substantially decreases inside the tube. In comparison to the walls of the tube, higher temperature exists in the center · We note that with higher the values of the Brinkman number, i.e. the ratio of viscous heat generation to external heating, the lesser will be the conduction of heat produced by viscous dissipation and hence larger the temperature rise see Fig.7(a-c). Temperature for Cu-water is observed to be higher as compared to pure water.

Figs. $7(a)-8(c)$ are prepared to analyze the entropy generation with respect to change in different physical constraints involved. Figs. $8(a)$ to $8(c)$ depict that entropy generation is directly proportional to Hartmann number, flow rate Q and ratio of Brinkman number Br with Λ , and that entropy generation for pure water is higher than that of Cu-water. It has larger values near the walls of the channel as compared to the center of the channel. It is to be noticed that for significantly larger values of these two parameters, entropy generation can be larger in the center of the tube than to those generated at the walls.

Figs. $9(a)-9(c)$ are prepared to analyze the Bejan number with respect to change in different physical constraints involved. Fig. $9(a)-9(c)$ depict that with the increase in Hartmann number, and flow rate ratio heat transfer irreversibility is high as compare to the total irreversibility due to heat transfer, fluid friction and magnetic field while results are opposite for the case of ratio of Brinkman number B_r with Λ.

Fig. 10 . Shows streamlines for different values of Hartmann number M for Copper water. It is seen that the size and number of trapped bolus increases for increasing M in upper part of the channel, while size of bolus decreases but number of bolus

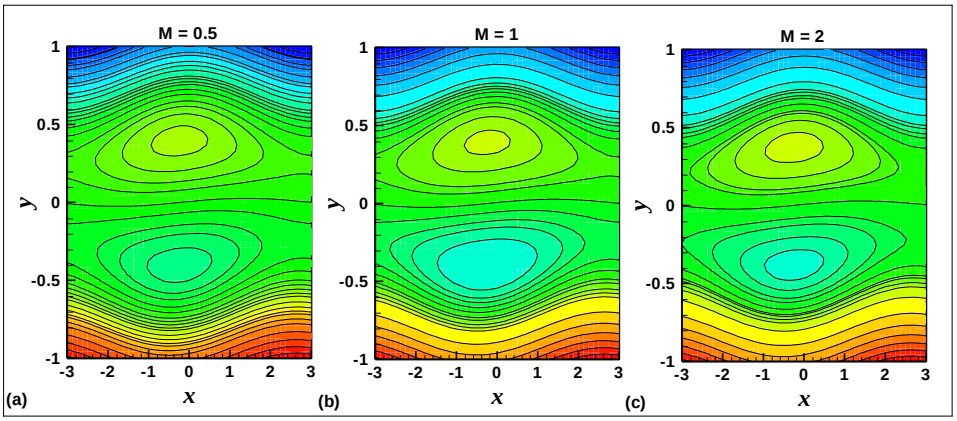

Fig. 10: Streamlines for different values of a) M=0.5, b) M=1 and M= 2 parameters for Copper water.

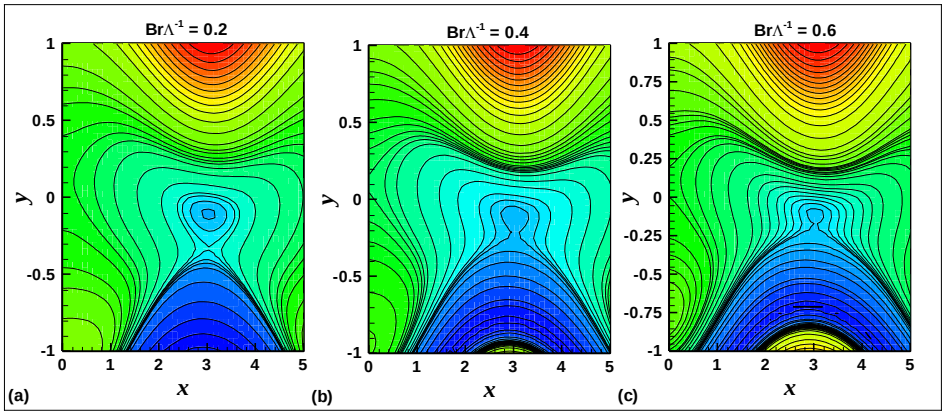

Fig. 11: Isotherms for a) BrΛ^{-1}=0.2, b) BrΛ^{-1}=0.4 and c) BrΛ^{-1}=0.6.

increases with the increase in Hartmann number M in lower part of the channel.

A line connecting points of equal temperature is called an isotherm. See Figs. 11, the small orange numbers are contour labels, which identify the value of an isotherm (75, 85 degrees Fahrenheit). So it analyzed that when we increases ratio of Brinkman number Br with Λ than temperature is 75, 85 degrees Fahrenheit.

CONCLUSION

This article is intended for investigating the entropy generation analysis for the peristaltic flow of Cu-water nanofluid with magnetic field. Key points of the present work are as follows.

1. We see that with the increase in the Hartmann number M, i.e. ratio of electromagnetic force to the viscous force, the velocity decreases in the center of the tube and increases near the walls of the tube, while as we increase the flow rate Q, the magnitude of velocity takes a positive shift all around the channel.

2. It is observed that Cu-water has more variation as that of pure water.

3. Temperature of the fluid in the channel significantly increases with an increase in flow rate Q and Brinkman number B_r and a decrease in Hartmann number M.

4. Entropy generation is directly proportional to Hartmann number, flow rate Q and ratio of Brinkman number Br with Λ, and that entropy generation for pure water is higher than that of Cu-water.

5. It is seen that the size and number of trapped bolus increases for increasing M in upper part of the channel, while size of bolus decreases but number of bolus increases with the increase in Hartmann number M in lower part of the channel.

6. It analyzed that when we increases ratio of Brinkman number Br with Λ than temperature is 75, 85 degrees Fahrenheit.

ACKNOWLEDGEMENTS

The Author is thankful to the Higher Education Commission Pakistan for the financial support to complete this work.

REFERENCES

Akbar, N. S. and S. Nadeem (2011). Endoscopic effects on the peristaltic flow of a nanofluid, Commun. *Theor. Phys*. 56, 761–768.

Akbar, N. S., Z. H. Khan and S. Nadeem (2014). Metachronal beating of cilia under influence of Hartmann layer and heat transfer, *Eur. Phys. J. Plus* 129, 176.

Akbar, N. S. (2015). Application of Eyring-Powell fluid model in peristalsis with nano particles. *Journal of computational and theoretical nanosciences* 12, 94-100.

Akbar, N. S. (2014). Biological analysis of nano Prandtl fluid model in a diverging tube. *Journal of computational and theoretical nanosciences* 12, 105-112.

Akbar, N. S. (2014). Peristaltic flow of Cu-water nanofluid in a tube. *Journal of computational and theoretical nanosciences* 11,1411–1416.

Akbar, N. S. and A. W. Butt (2015). Heat Transfer Analysis for the Peristaltic Flow of Herschel--Bulkley Fluid in a Nonuniform Inclined Channel. *Zeitschrift für Naturforschung A*. 70, 23-32.

Akbar, N. S. and S. Nadeem (2014). Convective heat transfer of a Sutterby fluid in an inclined asymmetric channel with partial slip. *Heat transfer research* 45(3), 219-240.

Akbar, N. S., S. Nadeem and Z. Hayat Khan (2014). The combined effects of slip and convective boundary conditions on stagnation-point flow of CNT suspended nanofluid over a stretching sheet. *Journal of Molecular Liquids* 196, 21–25.

Akbar, N. S., S. Nadeem, T. Hayat and A. Awatif Hendi (2012). Peristaltic flow of a nanofluid in a non-uniform tube. *Heat and Mass Transfer* 48, 451–459.

Akbar, N. S. and Z. H. Khan (2014). Heat transfer analysis of the peristaltic instinct of biviscosity fluid with the impact of thermal and velocity slips. *International Communications in Heat and Mass Transfer* 58, 193-199.

Anand, V. (2014). Slip law effects on heat transfer and entropy generation of pressure driven flow of a power law fluid in a microchannel under uniform heat flux boundary condition. *Energy* 76, 716–732.

Basak, T., R. Anandalakshmi, P. Kumar and S. Roy (2012). Entropy generation vs energy flow due to natural convection in a trapezoidal cavity with isothermal and non-isothermal hot bottom wall. *Energy* (37), 514-532.

Bejan, A. (1979). A study of entropy generation in fundamental convective heat transfer. *J. Heat Transfer* 101, 718–725.

Choi, S. U. S. (1995). Enhancing thermal conductivity of fluids with nanoparticles, in: D. A. Siginer, H. P. Wang (Eds.). *Developments and Applications of Non-Newtonian Flows*, , ASME, New York 66, 99–105.

Dagtekin, I., H. F. Oztop and A. Z. Sahin (2005). An Analysis of Entropy Generation through Circular Duct with Different Shaped Longitudinal Fins of Laminar Flow. *Int. J. Heat* Mass Transfer 48(1), 171–181.

Dagtekin, I., H. F. Oztop and A. Bahloul (2007). Entropy Generation for Natural Convection in <GAMMA>-Shaped Enclosures . *Int. Comm. Heat Mass Transfer* 34, 502–510.

Ebaid, A. (2008). A new numerical solution for the MHD peristaltic flow of a bio-fluid with variable viscosity in a circular cylindrical tube via Adomian decomposition method. *Physics Letters* A, 372, 5321-5328.

Ghasemi, J. and S. E. Razavi (2013). Numerical Nanofluid Simulation with Finite Volume Lattice-Boltzmann Enhanced Approach. *Journal of Applied Fluid Mechanics* 6, 519-527.

Ghatak, K. P., P. K. Bose, S. Bhattacharya, A. Bhattacharjee, D. De, S. Ghosh, S. Debbarma, and N. Paitya (2013). Simple Theoretical Analysis of the Fowler-Nordehim Field Emission from Quantum Confined Optoelectronic. *Materials Quantum Matter* 2, 83-101.

Guelpa, E., A. Sciacovelli and V. Verda (2013). Entropy generation analysis for the design improvement of a latent heat storage system. *Energy* 37, 128–138.

Hamad, M. A. A. and M. Ferdows (2012). Similarity solution of boundary layer stagnation-point flow towards a heated porous stretching sheet saturated with a nanofluid with heat absorption/generation and suction/blowing: a Lie group analysis. *Commun. in Nonlinear Sci. and Numerical Simulat* 17, 132–140.

Hamad, M. A. A. and M. Ferdows (2012). Similarity solutions to viscous flow and heat transfer of nanofluid over nonlinearly stretching sheet. *Appl. Math. Mech. -Engl. Ed*. 33(7), 923–930.

Hijleh, B. A., M. Abu-Qudais and E. Abu-Nada (2014). Numerical prediction of entropy generation due to natural convection from a horizontal cylinder. *Energy* 24, 27–333.

Keblinski, P. , S. R. Phillpot, S. U. S Choi and J. A Eastman (2002). Mechanisms of heat flow in suspensions of nano-sized particles. *Int. J. of*

Heat and Mass transfer $45,855-863$.

Latham, T. W. (1966). *Fluid motion in a peristaltic pump*, MS. Thesis, Massachusetts Institute of Technology, Cambridge.

Ma¨ga, S. E., S. J. Palm, C. T. Nguyen, G. Roy and N. Galanis (2005) . Heat transfer enhancement by using nanofluids in forced convection flows. *Int. J. of Heat and Fluid Flow*. 26, $530-546$.

Nada, E. A. (2006). Entropy generation due to heat and fluid flow in backward facing step flow with various expansion ratios. *Int. J. Exergy* 3, 4.

Oztop, H. F., A. Z. Sahin and I. Dagtekin (2004). Entropy Generation Through Hexagonal Cross-Sectional Duct for Constant Wall Temperature in Laminar Flow. *Int. J. Energy Res*., 28(8), $725-737$.

Oztop, H. F. and K. Al-Salem (2012). A Review on Entropy Generation in Natural and Mixed Convection Heat Transfer for Energy Systems. *Ren. Sust. En. Reviews* $16(1), 911-920$.

Pakdemirli, M. and B. S. Yilbas (2006) . Entropy generation in a pipe due to non-Newtonian fluid flow: Constant viscosity case. *Sadhana* 31, $21-29$.

Ramiar, A., A. A. Ranjbar and S. F.Hosseinizadeh, (2012) . Effect of Axial Conduction and Variable Properties on TwoDimensional Conjugate Heat Transfer of Al2O3-EG/Water Mixture Nanofluid in Microchannel. *Journal of Applied Fluid Mechanics* $5,79-87$.

Rashad, A. M., A. J. Chamkha and M. M. M. Abdou (2013). Mixed Convection Flow of Non-Newtonian Fluid from Vertical Surface Saturated in a Porous Medium Filled with a Nanofluid. *Journal of Applied Fluid Mechanics* 6, 301-309.